THE JOURNAL OF PHYSICAL CHEMISTRY Letters

Letter

pubs.acs.org/JPCL

One-Step Route to Luminescent $Au_{18}SG_{14}$ in the Condensed Phase and Its Closed Shell Molecular Ions in the Gas Phase

Atanu Ghosh, Thumu Udayabhaskararao, and Thalappil Pradeep*

DST Unit of Nanoscience (DST UNS) Department of Chemistry, Indian Institute of Technology Madras, Chennai 600 036, India

Supporting Information

ABSTRACT: We report a one-step route for the synthesis of highly luminescent and water-soluble $Au_{18}SG_{14}$ (SG- glutathione in thiolate form) in nearly pure form using a slow reduction process. The cluster shows step-like behavior in its absorption profile. It emits red light in both aqueous and solid state under UV illumination. Quantum yield of the cluster is 0.053, nearly 25-fold higher than that of $Au_{25}SG_{18}$. The cluster exhibits distinct features corresponding to multiply charged ions in electrospray ionization mass spectrometry. This composition is also confirmed from MALDI MS along with other quantitative analyses. The cluster makes closed shell molecular ions in the gas phase. The possibility of making clusters of different core sizes is also demonstrated. The simplicity of this method and identification of the cluster with exact composition may facilitate the exploration of experimental and theoretical research on this material.

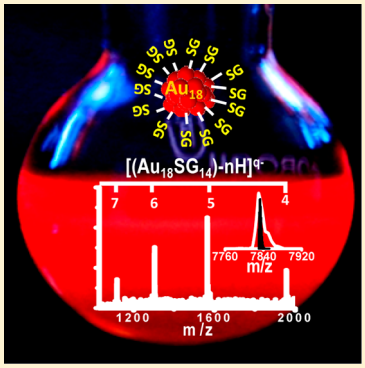

SECTION: Physical Processes in Nanomaterials and Nanostructures

Development of noble metal quantum clusters (QCs) of atomically precise composition[1−10] is necessary to explore their new applications in diverse areas such as catalysis,[11−15] biomedicine,[16−19] and nanoelectronics.[20] As properties of QCs vary with each atom added, it is important to obtain samples with high purity. However, several synthetic methods produce mixtures of clusters, and subsequent purification is necessary in order to separate a specific QC.[21] Direct synthesis of clusters of specific nuclearity in macroscopic quantities is important to understand their unique properties. Impressive achievements have been accomplished to obtain $Au_{25}SG_{18}$ (SG, glutathione thiolate) clusters directly by a variety of methods.[2,22,23] As a result, it is the most intensely studied cluster in this category.[22−28] However, single-step methods to make sizable quantities of specific Au_nSG_m (n = 10, 15, 18, 29, 33) clusters are yet to be developed so that their properties can be explored. Herein, we report a one-step route for the synthesis of an atomically precise cluster, $Au_{18}SG_{14}$ in the hundreds of milligrams scale. Besides characterizing the clusters by diverse tools, we examine their closed shell molecular ions in the gas phase. We show that the cluster ions with their monolayers behave similarly to closed-shell systems.[29,30]

We use the concept that the core sizes of the clusters are generally determined by the relative rates of nucleation and growth, controlled by the reducing capability of the reagent used. In organic synthesis, sodium cyanoborohydride ($NaBH_3CN$) is used as a mild and selective reducing agent, whereas the typical reagent, $NaBH_4$, is strong and less selective.[31] A mild and selective reducing agent can help slow down nucleation and retard the growth of the nuclei, which may result in the direct formation of smaller Au:SG QCs. Following this idea, an aqueous solution of $NaBH_3CN$ was injected rapidly into a methanolic solution of Au^{1+}-SG polymers (details in the methods section). The resulting precipitate was collected and washed repeatedly with methanol to remove the remaining starting precursors, yielding a clear solution showing well-defined optical absorption features (Figure 1A) and characteristic color (Figure 1B). Excitation and emission spectra of the solution are shown in the inset of Figure 1A. The solution was freeze-dried to get a pale red powder (insets of Figure 1B), characterized as $Au_{18}SG_{14}$. Purity of the cluster is the most important aspect of this direct synthesis.

Polyacrylamide gel electrophoresis (PAGE, details in the methods section) of the cluster showed principally one band (Figure 1C), which confirmed the formation of a single cluster. To ensure the absence of other clusters, high-resolution PAGE was performed with 35% gel concentration. However, we did not observe any additional band, suggesting that no other cluster was formed in detectable quantities. The formula, $Au_{18}SG_{14}$, and the purity of the QC were confirmed based on mass spectrometry (MS), including electrospray ionization (ESI) and matrix-assisted laser desorption ionization (MALDI) methods (presented below). The as-synthesized cluster is stable for months in the solid state as well as in the aqueous medium at ice-cold temperatures. The synthetic method is highly robust and is reproduced without adhering to stringent conditions of temperature, purity of materials, and so forth (which are

Received: June 7, 2012
Accepted: July 12, 2012

   dx.doi.org/10.1021/jz3007436 | J. Phys. Chem. Lett. 2012, 3, 1997−2002

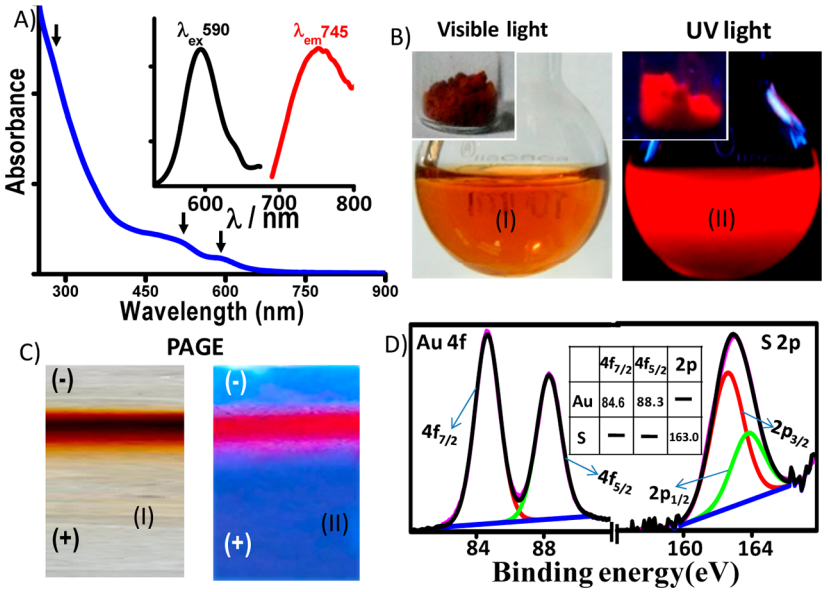

Figure 1. (A) UV−vis spectrum of the as-synthesized cluster. The spectrum shows dominant step-like behavior. Arrows indicate the well-defined optical features of the cluster. Inset: Luminescence spectrum (excitation and emission) of the cluster in water at 25 °C. (B) (I) photographs of the cluster solution in water and solid powder obtained by lyophilization of the solution (inset), in visible light, and (II) the same photographs under UV light. (C) (I) PAGE band of the cluster showing the presence of a single band, and (II) the same under UV light. The pink shade on either side of the band is due to the band edges with reduced concentration and not due to another cluster. (D) Photoelectron spectra of Au and sulfur with multiple components due to spin−orbit splitting. Peaks are fitted after background subtraction. Insets: Table presenting the BE values of gold and sulfur.

important in several QCs). The yield of the cluster in terms of Au is 61%, starting from 150 mg of $HAuCl_4{\cdot}3H_2O$. Note that the synthesis involves a lower Au:GSH (1:2.5) ratio than the standard (1:4) used to make a mixture of clusters.[22] The optical absorption spectrum of the as-prepared cluster shown in Figure 1A shows a step-like, multiple-band spectrum, which is usual for gold QCs. The most prominent absorption band is centered at 590 nm (2.1 eV); additional spectral features include a broad band at 515 nm (2.4 eV) and another band in the UV region at 290 nm (4.2 eV); all of these match with the recent results of Tlahuice and Garzon, who reported first-principle calculations on $Au_{18}SG_{14}$, according to which the Au_8 core is decorated by two −[S−Au−S−Au−S−Au−S]− and two −[S−Au−S−Au−S]− staples in the lowest energy structure.[32]The molecular orbitals responsible for optical transitions are not purely from the Au_8 core but formed due to the combination of atomic orbitals of Au_{core}, S, and Au_{staple}.[32] The higher wavelength peak at 590 nm is blue-shifted compared to Au_{25},[2] Au_{23},[33] Au_{22},[9] and Au_{20},[8] which show absorptions in the range of 600−800 nm, as expected from its smaller core size. Cluster in aqueous medium shows excitation at 590 nm (matching with the absorption maximum) and emission at 745 nm (insets of Figure 1A). $Au_{18}SG_{14}$ exhibits observable luminescence in the aqueous medium as well as in the solid state (images in Figure 1B). Cluster in the aqueous medium exhibits enhanced luminescence as compared to bigger QCs such as Au_{25}, where emission is difficult to be photographed in the aqueous medium. The measured quantum yield of the cluster is 5.3×10^{-2} at room temperature, using rhodamine 6G as the reference. This is ∼25-fold higher than that of $Au_{25}SG_{18}$ (quantum yield, 1.9×10^{-3}).[9]

All the expected elements are present in the cluster, which is confirmed from the XPS survey spectrum (Figure S1, Supporting Information). The binding energy (BE) is calibrated with respect to C1s at 284.6 eV. The photoelectron spectra in the Au 4f and S 2p regions are presented in Figure 1D. The expected Au $4f_{7/2}$ BEs of the Au(I)−thiolate complex and Au(0) film are 86.0 and 84.0 eV, respectively. The measured Au $4f_{7/2}$ BE of the cluster is 84.6 eV. This suggests the presence of a nearly Au(0) core, which is expected for smaller gold clusters.[9,21] The S $2p_{3/2}$ BE is 163.0 eV, characteristic of thiolate ligand. It is important to note that the luminescent Au_{18} thiacrown ether and similar systems are different from the present cluster, and they belong to the category of metal complexes.[34,35] Au_{18} thiacrown gave absorption features at 328 and 346 nm and emission at 500 nm.[34] As the core dimension is small, the clusters appear as tiny dots of <1 nm and are barely observable in transmission electron microscopy (TEM). Upon longer electron beam irradiation, they aggregate to form nanoparticles (Figure S2), which is already known in the case of clusters.[36,37]

For finding the molecular formula of the cluster, we used ESI MS. A 50% (v/v) water/methanol solution of the as-prepared cluster with a concentration of 0.1 mg/mL was used for ESI. At higher capillary temperatures, dissociation of the intact cluster into smaller fragments occurred, and species such as $[Au(SG)\text{-}H]^{1-}$ and $[Au_2(SG)_2\text{-}H]^{1-}$ were observed. In order to obtain the spectrum, an optimized capillary temperature (ca. 150 °C) was applied so that efficient solvent evaporation took place, leading to the formation of desolvated clusters in larger numbers.[21] Detailed mass analyses were conducted with ESI MS to know the composition of the cluster. It is known that Au:SG cluster contains negative charge in the aqueous state since most of the carboxyl groups of the GSH ligands tend to be dissociated. The acid dissociation constants of the two carboxyl groups of free GSH are 2.56 and 3.50.[38] As expected, the negative-ion ESI mass spectrum is comprised of a series of peaks associated with multiply charged anions due to the presence of the cluster (Figure 2). From an analysis of the mass spectrum, a chemical composition of $[Au_{18}SG_{14}\text{-}nH]^{q-}$ could be assigned for the molecular species obtained in this synthesis,

dx.doi.org/10.1021/jz3007436 | J. Phys. Chem. Lett. 2012, 3, 1997−2002

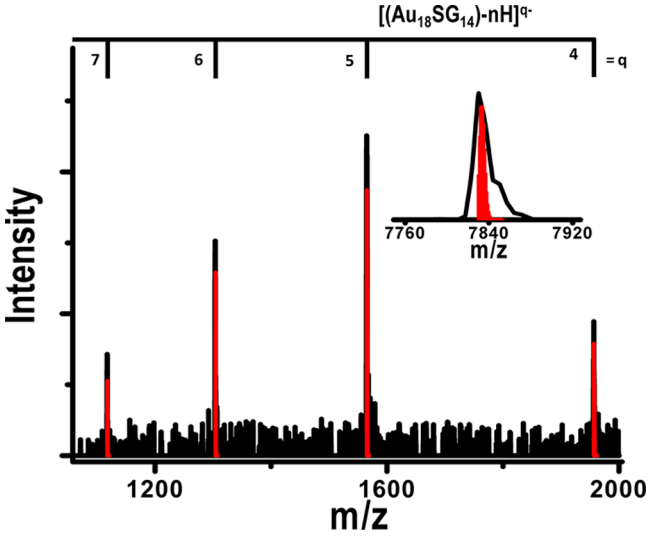

Figure 2. ESI MS spectrum of $Au_{18}SG_{14}$ in the negative mode, in the region of m/z 1000−2000. The peaks observed are due to $[Au_{18}SG_{14}\text{-}nH]^{q-}$, where n is the number of protons ionized from the carboxylic acid groups. The label q is the charge carried by the cluster. Red lines represent the calculated values for the given charge states. Inset shows the deconvoluted spectrum based on the multiply charged species observed. Besides the molecular ion feature at m/z 7830, it shows higher mass number shoulders due to sodium addition. In the spectra, the red spectrum in the inset gives the expected isotope distribution.

where n represents the number of dissociated protons, and q represents the charge of the cluster. Experimental distribution of multiply charged peaks matches perfectly with the expected pattern. Mass spectral peaks appear at the calculated positions. For example, the peaks due to $[Au_{18}(SG)_{14}\text{-}nH]^{q-}$ are at m/z 1956.2, 1565.2, 1304.3, and 1117.4 for q = 4, 5, 6 and 7, respectively. The peaks match with the calculated isotope pattern as well, although the instrumental resolution is not adequate to resolve the components of the multiply charged structure (Figure S3A). Deconvoluted spectrum shown in the inset of Figure 2 matches with the mass of $Au_{18}SG_{14}$. The deconvoluted spectrum of the whole mass spectrum is shown in Figure S3B, which also proves that only $Au_{18}SG_{14}$ is formed in the crude. No other clusters were detected. Deconvoluted spectrum was obtained using MagTran software.

MS analysis was carried out using MALDI as well. The matrix α-cyano-4-hydroxycinnamic acid (CHCA) was used. The spectrum collected in the positive mode shows a bunch of peaks with m/z values ranging from 100 to 10 000 (Figure S4A). Peaks at low m/z regions are very intense with huge background signals compared to those at higher m/z values. There is a pattern of peaks between m/z 1800 and 5400, and another pattern from m/z 5500 to 10 000. The second set of peaks is attributed to clustering of ions detected in the lower m/z values. Clustering of clusters is observed in MALDI MS studies of clusters.[39] The mass spectrum is composed of several groups of peaks with spacing of m/z 197 or 229 between the major peaks, as shown in Figure S4B. These correspond to the loss of Au (197) or AuS (229). The m/z spacing between isolated peaks is 32 on account of sulfur (Figure S4C). These results are consistent with the earlier reports of laser-desorption MS of gold QCs protected with thiolates.[9,33,40] Each bunch of peaks can be assigned as $[Au_mS_n]^+$. Since laser irradiation, especially at high laser powers can cleave the S−C bond of the ligands, we observe only peaks due to Au_m cores covered with S, and not the entire ligand. The mass spectrum showed a highest intense peak at m/z 3962. The peak matches with $Au_{18}S_{13}^+$ showing the presence of the Au_{18} core. In laser desorption experiments, some ligand loss (especially the bridged ones) is expected as in the case of Au_{25}, apart from the S−C bond cleavage, and as a result, $Au_{25}S_{12}$ is seen as the maximum intense feature in the spectrum of $Au_{25}SG_{18}$.[23] Intact molecular ions are difficult to see in water-soluble clusters, unlike in the case of organic soluble ones.

The Au:S ratio in the as-synthesized cluster powder using energy-dispersive analysis of X-rays (EDAX) (1:0.76) further supports the assignment of $Au_{18}SG_{14}$ (expected Au:S = 1:0.78) (Figure S5). The ligation of glutathione in the form of thiolate (SG) attached to the Au core was confirmed by the absence of the thiolate stretching peak at 2526 cm^{-1} in the Fourier transform infrared (FT-IR) spectrum of the cluster (Figure S6).

^1H NMR spectra of GSH and $Au_{18}SG_{14}$ were measured in D_2O, and the spectra are shown in Figure S7. The strong signal at 4.75 ppm arises due to the presence of residual water in D_2O. The H-7 (α-CH_2) and H-6 (β-CH_2) protons are very close to the gold core. For this reason, these proton signals shifted more downfield. The signal for H-7 became very broad (and not resolvable) and the signal corresponding to H-6 merged with the strong water signal.[23]

While exploring the mass spectrum of $Au_{18}SG_{14}$, one aspect of its electronic stability became apparent. Many of the ions observed are closed shell electron species as in the case of $[Au_{18}SG_{14}]^{4-}$. Increased stability of closed shell ions is exhibited in the mass spectrometry/mass spectrometry (MS/MS) studies of many of the charged species. Table 1 below lists all the ions satisfying the above case. MS/MS of $Au_{25}(SCH_2CH_2Ph)_{18}$ was reported earlier.[41]

MS/MS of m/z 1956 (4− charge) gave fragment ion peaks with a separation of m/z 32.5. Therefore, the actual mass loss is 32.5 × 4 = 130. The only possibility to have this loss is the fragmentation of glutathione, which is a tripeptide of glutamic acid, cysteine, and glycine. There are two possibilities for it to fragment, namely, at the two peptide bonds. Among them, the

Table 1. All the Ions Formed during (MS/MS) Analysis[a]

cluster formula	m	n	q	$m - n + q$
$[Au_{18}SG_{14}]^{4-}$	18	14	4	8
$[Au_{18}SG_{13}SG_F]^{4-}$	18	14	4	8
$[Au_{18}SG_{13}SG_F\text{-}H_2O]^{4-}$	18	14	4	8
$[Au_{18}SG_{12}(SG_F)_2]^{4-}$	18	14	4	8
$[Au_{18}SG_{12}(SG_F)_2\text{-}H_2O]^{4-}$	18	14	4	8
$[Au_{18}SG_{11}(SG_F)_3]^{4-}$	18	14	4	8
$[Au_{18}SG_{11}(SG_F)_3\text{-}H_2O]^{4-}$	18	14	4	8
$[Au_{18}SG_{10}(SG_F)_4]^{4-}$	18	14	4	8
$[Au_{18}SG_{10}(SG_F)_4\text{-}H_2O]^{4-}$	18	14	4	8
$[Au_{17}SG_{13}]^{4-}$	17	13	4	8
$[Au_{17}SG_{12}(SG_F)]^{4-}$	17	13	4	8
$[Au_{16}SG_{12}]^{4-}$	16	12	4	8
$[Au_{16}SG_{11}(SG_F)]^{4-}$	16	12	4	8
$[Au_{15}SG_{11}]^{4-}$	15	11	4	8
$[Au_{14}SG_{10}]^{4-}$	14	10	4	8
$[Au_{12}SG_8]^{4-}$	12	8	4	8

[a]Total electron count ($m - n + q$) shows that all the ions contain $8e^-$, i.e., they are forming closed shell molecular ions in the gas phase. Here m, n, and q represent the number of gold atoms, thiolated ligands, and charges on the ligand. The electron counting rule includes the charges on the ligand also.

dx.doi.org/10.1021/jz3007436 | J. Phys. Chem. Lett. 2012, 3, 1997−2002

fragmentation between glutamic acid and cysteine is facile. Cleavage at $C_{glutamic\ acid}$—$N_{cysteine}$ produces two fragments of m/z 130 ($C_5H_8O_3N$) and 176 ($C_5H_8O_3N_2S$). The fragment m/z 176 contains the thiol group, and therefore it got attached with the cluster and the other leaves. The $C_5H_8O_3N_2S$ fragment is labeled SG_F.

$$[Au_{18}SG_{14}]^{4-} \rightarrow [Au_{18}SG_{13}SG_F]^{4-} + C_5H_8O_3N$$

There was systematic loss of $C_5H_8O_3N$ as the collision energy was increased (Figure 3). Along with each fragmented peak,

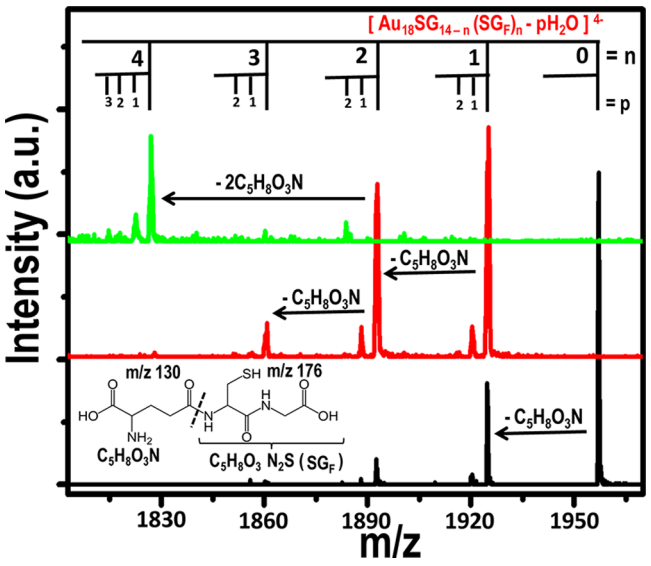

Figure 3. MS/MS spectra of $[Au_{18}SG_{14}]^{4-}$ with increasing collision energy. Here n represents the number of glutathione ligands fragmented and p represents the number of water losses. Inset shows the fragmentation channel of glutathione. The mass spectra from bottom to top are with increasing collision energy.

one more peak with m/z 4.5 loss was also observed. This loss ($4.5 \times 4 = 18$) corresponds to H_2O, as shown in Figure 3, indicating that glutathione existed as an anhydride at the cluster surface (a schematic of anhydride formation is shown in Figure S8). With increasing collision energy, the fragments so formed, derived from amide bond cleavage of glutathione, further lose water, producing a series of pH_2O losses (p = 1, 2,..).

It was observed that there was no water loss from the unfragmented ion, $[Au_{18}SG_{14}]^{4-}$. After fragmentation of one glutathione group, it forms $[Au_{18}SG_{13}(SG_F)]^{4-}$, from which water loss started. It is likely that after fragmentation, some structural change happens on the cluster surface, which assisted the water loss. At higher collision energy, a loss of 4 $C_5H_8O_3N$ is observed.

At the same time, we have observed weak peaks at m/z 503 and 1006, which are due to the loss of AuSG (197 + 306) and Au_2SG_2 ($197 \times 2 + 306 \times 2$) (Figure S8). The ion Au_2SG_2 is prominent at a certain collision energy. The resultant peak upon loss of AuSG and Au_2SG_2 from $[Au_{18}SG_{13}SG_F]^{4-}$ (m/z 1924.3) gives ions at m/z 1799.0 and 1674.1, respectively corresponding to $[Au_{17}SG_{12}SG_F]^{4+}$ and $[Au_{16}SG_{11}SG_F]^{4+}$. A peak at m/z 1704.9 appeared due to the formation of $[Au_{16}SG_{12}]^{4-}$ from $[Au_{18}SG_{14}]^{4-}$ (Figure S9). This is contrary to the data at low collision energies, where fragmentation happened from the already fragmented species $[Au_{18}SG_{13}SG_F]^{4-}$; but it happened from the parent cluster $[Au_{18}SG_{14}]^{4-}$ itself in the present case. The same trend was continued for higher collision energies also. No other fragments with other charge species except 4− were observed in the MS/MS spectrum. All these species observed correspond to $m - n + q = 8$, where m is the number of gold atoms, n is the number of thiolate ligands, and q is the charge on the ligand. This increased stability of 8e- fragments is seen if we start from other ions as well, which are not $8e^-$ species to begin with. For example, $[Au_{18}SG_{14}]^{5-}$ produces a 4− species upon increasing the collision energy (Figure S9). Similar "charge stripping" is seen with other anions as well, as shown in Figures S10 and S11. This kind of ion formation suggests increased stability of the tetra anion. We believe that these results closely resemble the increased stability of the Jellium core.[30] However, in the present case, the electron count includes the charges on the ligands as well. Table 1 in the Supporting Information presents the calculated and experimental masses of the ions observed, and Table 2 presents the calculated mass of the cluster based on the ion masses.

Variation of the concentration of $NaBH_3CN$ in the synthesis produces other clusters. For example, Figure S12 compares the UV spectra of three different samples prepared by the addition of different concentrations of $NaBH_3CN$ to Au(I) glutathione solution at a Au:GSH molar ratio of 1:2.5. It is clear that various concentrations of the reducing agent can give different QCs of gold, although optimization is necessary to make one specific core. Close inspection of Figure S12 shows that the absorption band maxima associated with the Au 6sp intraband transitions are shifted systematically with change in core size.

In summary, a novel route to produce $Au_{18}SG_{14}$ is reported. We have made a highly pure and stable material, in large quantities by the appropriate choice of synthetic parameters. Since these clusters are highly fluorescent and biocompatible due to the lower metallic content, they hold great promise as ultrabright, biocompatible biolabels and light-emitting sources at the nanoscale. These clusters can be readily conjugated with several biological molecules, which further enhances their application potential. We believe that essential properties of $Au_{18}SG_{14}$ reported here will generate further interest in this class of materials. One-step synthesis of this material in large quantities will enable the exploration of its properties. We performed MS/MS of $Au_{18}SG_{14}$, which confirms that the observed ions in the gas phase satisfy the model of closed electronic shell. We show that it is possible to make several other clusters of well-defined composition by the same route. The factors responsible for selective formation of $Au_{18}SG_{14}$ need additional studies.

■ ASSOCIATED CONTENT

Ⓢ Supporting Information

Figures S1−S12 and Tables 1−2. This material is available free of charge via the Internet at http://pubs.acs.org.

■ AUTHOR INFORMATION

Corresponding Author

*E-mail: pradeep@iitm.ac.in.

Notes

The authors declare no competing financial interest.

■ ACKNOWLEDGMENTS

We thank the Department of Science and Technology, Government of India, for constantly supporting our research program on nanomaterials.

■ REFERENCES

(1) Jadzinsky, P. D.; Calero, G.; Ackerson, C. J.; Bushnell, D. A.; Kornberg, R. D. Structure of a Thiol Monolayer-Protected Gold Nanoparticle at 1.1 Å Resolution. *Science* **2007**, *318*, 430−433.

(2) Shichibu, Y.; Negishi, Y.; Tsukuda, T.; Teranishi, T. Large-Scale Synthesis of Thiolated Au25 Clusters via Ligand Exchange Reactions of Phosphine-Stabilized Au_{11} Clusters. *J. Am. Chem. Soc.* **2005**, *127*, 13464−13465.

(3) Nimmala, P. R.; Dass, A. $Au_{36}(SPh)_{23}$ Nanomolecules. *J. Am. Chem. Soc.* **2011**, *133*, 9175−9177.

(4) Zheng, J.; Petty, J. T.; Dickson, R. M. High Quantum Yield Blue Emission from Water-Soluble Au_8 Nanodots. *J. Am. Chem. Soc.* **2003**, *125*, 7780−7781.

(5) Wu, Z.; MacDonald, M. A.; Chen, J.; Zhang, P.; Jin, R. Kinetic Control and Thermodynamic Selection in the Synthesis of Atomically Precise Gold Nanoclusters. *J. Am. Chem. Soc.* **2011**, *133*, 9670−9673.

(6) Rao, T. U. B.; Nataraju, B.; Pradeep, T. Ag_9 Quantum Cluster through a Solid-State Route. *J. Am. Chem. Soc.* **2010**, *132*, 16304−16307.

(7) Levi-Kalisman, Y.; Jadzinsky, P. D.; Kalisman, N.; Tsunoyama, H.; Tsukuda, T.; Bushnell, D. A.; Kornberg, R. D. Synthesis and Characterization of $Au_{102}(p\text{-}MBA)_44$ Nanoparticles. *J. Am. Chem. Soc.* **2011**, *133*, 2976−2982.

(8) Zhu, M.; Qian, H.; Jin, R. Thiolate-Protected Au20 Clusters with a Large Energy Gap of 2.1 eV. *J. Am. Chem. Soc.* **2009**, *131*, 7220−7221.

(9) Shibu, E. S.; Radha, B.; Verma, P. K.; Bhyrappa, P.; Kulkarni, G. U.; Pal, S. K.; Pradeep, T. Functionalized Au_{22} Clusters: Synthesis, Characterization, and Patterning. *ACS Appl. Mater. Interfaces* **2009**, *1*, 2199−2210.

(10) Shibu, E. S.; Pradeep, T. Quantum Clusters in Cavities: Trapped Au_{15} in Cyclodextrins. *Chem. Mater.* **2011**, *23*, 989−999.

(11) Arenz, M.; Landman, U.; Heiz, U. CO Combustion on Supported Gold Clusters. *Chem. Phys. Chem.* **2006**, *7*, 1871−1879.

(12) Liu, Y.; Tsunoyama, H.; Akita, T.; Tsukuda, T. Efficient and Selective Epoxidation of Styrene with TBHP Catalyzed by Au25 Clusters on Hydroxyapatite. *Chem. Commun.* **2010**, *46*, 550−552.

(13) Leelavathi, A.; Bhaskara Rao, T.; Pradeep, T. Supported Quantum Clusters of Silver as Enhanced Catalysts for Reduction. *Nanoscale Res. Lett.* **2011**, *6*, 1−9.

(14) Zhu, Y.; Qian, H.; Drake, B. A.; Jin, R. Atomically Precise $Au_{25}(SR)_{18}$ Nanoparticles as Catalysts for the Selective Hydrogenation of α,β-Unsaturated Ketones and Aldehydes. *Angew. Chem., Int. Ed.* **2010**, *49*, 1295−1298.

(15) de Silva, N.; Ha, J.-M.; Solovyov, A.; Nigra, M. M.; Ogino, I.; Yeh, S. W.; Durkin, K. A.; Katz, A. A Bioinspired Approach for Controlling Accessibility in Calix[4]arene-Bound Metal Cluster Catalysts. *Nat. Chem.* **2010**, *2*, 1062−1068.

(16) Polavarapu, L.; Manna, M.; Xu, Q.-H. Biocompatible Glutathione Capped Gold Clusters As One- and Two-Photon Excitation Fluorescence Contrast Agents for Live Cells Imaging. *Nanoscale* **2011**, *3*, 429−434.

(17) Habeeb Muhammed, M. A.; Verma, P. K.; Pal, S. K.; Retnakumari, A.; Koyakutty, M.; Nair, S.; Pradeep, T. Luminescent Quantum Clusters of Gold in Bulk by Albumin-Induced Core Etching of Nanoparticles: Metal Ion Sensing, Metal-Enhanced Luminescence, and Biolabeling. *Chem.—Eur. J.* **2010**, *16*, 10103−10112.

(18) Gobin, A. M.; Lee, M. H.; Halas, N. J.; James, W. D.; Drezek, R. A.; West, J. L. Near-Infrared Resonant Nanoshells for Combined Optical Imaging and Photothermal Cancer Therapy. *Nano Lett.* **2007**, *7*, 1929−1934.

(19) Ray, P. C.; Khan, S. A.; Singh, A. K.; Senapati, D.; Fan, Z. Nanomaterials for Targeted Detection and Photothermal Killing of Bacteria. *Chem. Soc. Rev.* **2012**, *41*, 3193−3209.

(20) Sivaramakrishnan, S.; Chia, P.-J.; Yeo, Y.-C.; Chua, L.-L.; Ho, P. K. H. Controlled insulator-to-metal transformation in printable polymer composites with nanometal clusters. *Nat. Mater.* **2007**, *6*, 149−155.

(21) Negishi, Y.; Nobusada, K.; Tsukuda, T. Glutathione-Protected Gold Clusters Revisited: Bridging the Gap between Gold(I)−Thiolate Complexes and Thiolate-Protected Gold Nanocrystals. *J. Am. Chem. Soc.* **2005**, *127*, 5261−5270.

(22) Shibu, E. S.; Muhammed, M. A. H.; Tsukuda, T.; Pradeep, T. Ligand Exchange of $Au_{25}SG_{18}$ Leading to Functionalized Gold Clusters: Spectroscopy, Kinetics, and Luminescence. *J. Phys. Chem. C* **2008**, *112*, 12168−12176.

(23) Wu, Z.; Gayathri, C.; Gil, R. R.; Jin, R. Probing the Structure and Charge State of Glutathione-Capped $Au_{25}(SG)_{18}$ Clusters by NMR and Mass Spectrometry. *J. Am. Chem. Soc.* **2009**, *131*, 6535−6542.

(24) Parker, J. F.; Fields-Zinna, C. A.; Murray, R. W. The Story of a Monodisperse Gold Nanoparticle: $Au_{25}L_{18}$. *Acc. Chem. Res.* **2010**, *43*, 1289−1296.

(25) Habeeb Muhammed, M. A.; Pradeep, T. Au_{25}@SiO2: Quantum Clusters of Gold Embedded in Silica. *Small* **2011**, *7*, 204−208.

(26) Hamouda, R.; Bellina, B.; Bertorelle, F.; Compagnon, I.; Antoine, R.; Broyer, M.; Rayane, D.; Dugourd, P. Electron Emission of Gas-Phase $[Au_{25}(SG)_{18}\text{-}6H]^{7-}$ Gold Cluster and Its Action Spectroscopy. *J. Phys. Chem. Lett.* **2010**, *1*, 3189−3194.

(27) Kumar, S. S.; Kwak, K.; Lee, D. Amperometric Sensing Based on Glutathione Protected Au_{25} Nanoparticles and Their pH Dependent Electrocatalytic Activity. *Electroanalysis* **2011**, *23*, 2116−2124.

(28) Shichibu, Y.; Negishi, Y.; Tsunoyama, H.; Kanehara, M.; Teranishi, T.; Tsukuda, T. Extremely High Stability of Glutathionate-Protected Au_{25} Clusters Against Core Etching. *Small* **2007**, *3*, 835−839.

(29) de Heer, W. A. The Physics of Simple Metal Clusters: Experimental Aspects and Simple Models. *Rev. Mod. Phys.* **1993**, *65*, 611−676.

(30) Hakkinen, H. Atomic and Electronic Structure of Gold Clusters: Understanding Flakes, Cages and Superatoms from Simple Concepts. *Chem. Soc. Rev.* **2008**, *37*, 1847−1859.

(31) Borch, R. F.; Bernstein, M. D.; Durst, H. D. Cyanohydridoborate Anion as a Selective Reducing Agent. *J. Am. Chem. Soc.* **1971**, *93*, 2897−2904.

(32) Tlahuice, A.; Garzon, I. L. On the Structure of the $Au_{18}(SR)_{14}$ Cluster. *Phys. Chem. Chem. Phys.* **2012**, *14*, 3737−3740.

(33) Muhammed, M. A. H.; Verma, P. K.; Pal, S. K.; Kumar, R. C. A.; Paul, S.; Omkumar, R. V.; Pradeep, T. Bright, NIR-Emitting Au_{23} from Au_{25}: Characterization and Applications Including Biolabeling. *Chem.—Eur. J.* **2009**, *15*, 10110−10120.

(34) Lee, T. K.-M.; Zhu, N.; Yam, V. W.-W. An Unprecedented Luminescent Polynuclear Gold(I) μ3-Sulfido Cluster with a Thiacrown-like Architecture. *J. Am. Chem. Soc. 132*, 17646-17648.

(35) Yam, V. W.-W.; Yip, S.-K.; Yuan, L.-H.; Cheung, K.-L.; Zhu, N.; Cheung, K.-K. Synthesis, Structure, and Ion-Binding Properties of Luminescent Gold(I) Alkynylcalix[4]crown-5 Complexes. *Organometallics* **2003**, *22*, 2630−2637.

(36) Udaya Bhaskara Rao, T.; Pradeep, T. Luminescent Ag_7 and Ag_8 Clusters by Interfacial Synthesis. *Angew. Chem., Int. Ed.* **2010**, *49*, 3925−3929.

(37) Ramasamy, P.; Guha, S.; Shibu, E. S.; Sreeprasad, T. S.; Bag, S.; Banerjee, A.; Pradeep, T. Size Tuning of Au Nanoparticles Formed by Electron Beam Irradiation of Au_{25} Quantum Clusters Anchored within and outside of Dipeptide Nanotubes. *J. Mater. Chem.* **2009**, *19*, 8856−8462.

(38) Takehara, K.; Ide, Y.; Aihara, M.; Obuchi, E. An Ion-Gate Response of the Glutathione Monolayer Assembly Formed on a Gold Electrode: Part 1. The Effect of pH, K^+ and Ca^{2+}. *Bioelectrochem. Bioenerg.* **1992**, *29*, 103−111.

(39) Cyriac, J.; Rajeev Kumar, V. R.; Pradeep, T. Gas Phase Aggregates of Protected Clusters. *Chem. Phys. Lett.* **2004**, *390*, 181−185.
(40) Schaaff, T. G. Laser Desorption and Matrix-Assisted Laser Desorption/Ionization Mass Spectrometry of 29-kDa Au:SR Cluster Compounds. *Anal. Chem.* **2004**, *76*, 6187−6196.
(41) Angel, L. A.; Majors, L. T.; Dharmaratne, A. C.; Dass, A. Ion Mobility Mass Spectrometry of $Au_{25}(SCH_2CH_2Ph)_{18}$ Nanoclusters. *ACS Nano* **2010**, *4*, 4691−4700.